DTU Library

Ultra-Wideband Coplanar Waveguide to Asymmetric Coplanar Stripline Transition from DC to 165 GHz

Dong, Yunfeng; Johansen, Tom Keinicke; Zhurbenko, Vitaliy

Published in:
International Journal of Microwave and Wireless Technologies

Link to article, DOI:
10.1017/S175907871800082X

Publication date:
2018

Document Version
Peer reviewed version

International Journal of Microwave and Wireless Technologies

cambridge.org/mrf

Ultra-wideband coplanar waveguide-to-asymmetric coplanar stripline transition from DC to 165 GHz

Yunfeng Dong[1], Tom K. Johansen[1] and Vitaliy Zhurbenko[1]

[1]Electromagnetic Systems Group, Department of Electrical Engineering, Technical University of Denmark, Oersteds Plads Building 348, 2800 Kgs. Lyngby, Denmark

Research Paper

Cite this article: Dong Y, Johansen TK, Zhurbenko V (2018). Ultra-wideband coplanar waveguide-to-asymmetric coplanar stripline transition from DC to 165 GHz. *International Journal of Microwave and Wireless Technologies* 1–7. https://doi.org/10.1017/S175907871800082X

Received: 14 August 2017
Revised: 1 May 2018
Accepted: 7 May 2018

Keywords:
passive components and circuits; terahertz technology and applications; wideband transition

Author for correspondence: Yunfeng Dong, E-mail: yundon@elekro.dtu.dk

Abstract

This paper presents an ultra-wideband coplanar waveguide (CPW)-to-asymmetric coplanar stripline (ACPS) transition based on aluminum nitride (AlN) substrate. The concepts of designing CPW, ACPS, and CPW-to-ACPS transition are explained. In order to suppress parasitic modes, vias going through AlN substrate are added along the ground traces. The signal trace is tapered out and chamfered to reduce the reflection caused by the termination of ground trace. The CPW-to-ACPS transition is designed, fabricated, and measured in a back-to-back configuration. The fabricated CPW-to-ACPS transition can provide a bandwidth of 165 GHz with an associated insertion loss of 3 dB.

Introduction

Transitions are necessary when different types of transmission lines are connected to each other. For designing wideband transitions, not only the characteristic impedances but also the propagation modes between the connected transmission lines need to be matched. With carefully designed transitions, the electromagnetic waves can be guided smoothly through different structures and the propagation mode is converted. The mismatch of either characteristic impedance or propagation mode result in a narrowband transition with high insertion loss [1]. Transmission lines such as microstrip line, coplanar waveguide (CPW), coplanar stripline (CPS), and asymmetric coplanar stripline (ACPS) used for microwave integrated circuits (MICs) as well as monolithic microwave integrated circuits (MMICs) mainly rely on planar structures due to their fabrication processes. Compared with microstrip line, CPW, and CPS have low transmission loss and their characteristic impedances are less sensitive to the thickness of the substrate which makes it possible to taper the dimensions of the transmission lines without affecting the characteristic impedance. It also makes CPW and CPS versatile for designing components and chips based on different substrates and packaging them into a system. In communication systems, CPW in a ground-signal-ground (GSG) configuration is normally used for designing amplifiers [2–5], frequency doublers [6, 7], mixers [8, 9], power digital to analog converters [10, 11], and interposer connections between different components [12, 13]. Being different from CPW, CPS as well as ACPS are in a ground-signal (GS) configuration and they are used for designing baluns [14–17], antennas [18–20], and the electrodes of Mach-Zehnder modulators (MZMs) [21–23].

For system integrations, it becomes critical for connecting the output of a driver to the input of a MZM or designing an on-chip dipole antenna at the output of a power amplifier. Under these circumstances, the transitions between GSG and GS are necessary. With the ever increasing demand worldwide for high-speed communication, the ultra-wideband transitions between different types of planar transmission lines with the ability of supporting transmissions from DC to terahertz (THz) frequencies are under intensive study. The challenges in designing wideband transitions include characteristic impedance mismatch, mode conversion loss, resonance, and radiation. Several publications can be found for CPW-to-microstrip [24, 25], CPW-to-stripline [26, 27], and CPW-to-CPS [18, 28, 29] transitions while rarely for CPW-to-ACPS transitions. A transition between CPW and CPS used for feeding a multiband dipole antenna was published in [18]. By using wire bonding bridges, the proposed CPW-to-CPS transition based on silicon substrate achieves a bandwidth up to 55 GHz. In [28], the designed CPW-to-CPS transition based on aluminum nitride (AlN) substrate with wire bonding bridges can support transmissions from DC to 80 GHz which is used for feeding an indium phosphide (InP) MZM. According to [29], by using reformed air-bridge the demonstrated CPW-to-CPS transition based on gallium arsenide (GaAs) substrate exhibits a bandwidth up to 110 GHz.

The purpose of this paper is to introduce an ultra-wideband CPW-to-ACPS transition based on AlN substrate which can be used as an interposer connection between a driver and an InP MZM. The concepts of designing CPW, ACPS, and CPW-to-ACPS transition are explained. The effect of adding vias all the way along the ground traces is also discussed. The design of CPW-to-ACPS transition with vias going through AlN substrate is demonstrated in detail and the magnitude of electric field distributions at different cross-sections of the transition are illustrated. The proposed CPW-to-ACPS transition is fabricated and measured in a back-to-back configuration. The simulation and measurement results are compared. To the best of our knowledge, the proposed CPW-to-ACPS transition with vias achieves the largest bandwidth ranging from DC to 165 GHz.

CPW and ACPS design considerations

CPW with vias

For a conventional CPW, two ground traces are located alongside the signal trace forming a GSG structure and a quasi-transverse electromagnetic mode can be supported. Since the characteristic impedance of a CPW is mainly determined by the width of the signal trace and the width of the gaps between the signal and ground traces, the same characteristic impedance can be achieved by CPWs with different dimensions on the same substrate. Though the ground traces play a minor role in affecting the characteristic impedance, it has to be wide enough in order to support the propagation mode since the electromagnetic waves mainly exist in the gaps. The CPW with vias based on AlN substrate shown in Fig. 1 is designed as a part of the CPW-to-ACPS transition.

The characteristic impedance of the CPW is designed to be 50 Ω based on AlN substrate with a thickness of 127 μm. The dielectric constant (ϵ_r) and dissipation factor (tanδ) of the substrate are 8.6 and 0.001, respectively. There are two conductor layers where the CPW is patterned on the top layer and the bottom layer works as a ground plane. The conductor is gold and the skin depth is calculated to be 0.18 μm at 170 GHz. In order to guarantee reasonable performances at low frequencies, the thickness of the conductor layers is designed to be 1.2 μm. Unlike conventional CPW structure, hollow plated vias are added along the ground traces going through the substrate and connecting the ground traces on the top to the ground plane on the bottom. The vias plated with gold are placed as close to the gaps as possible and the ground traces are designed as narrow as possible in order to suppress parasitic modes. Due to fabrication limitations, the diameter of the vias cannot be smaller than the thickness of the substrate and the edge of the vias should be at least 63.5 μm away from the edge of the conductor. As a result, for the designed CPW with vias, the width of the signal trace is 60 μm and the width of the ground trace is 254 μm with a gap width of 34 μm. The diameter of the vias is 127 μm and the center-to-center distance between two vias is 254 μm. The length and width of the substrate are 1.524 and 1.4 mm, respectively.

The designed CPW with vias is analyzed using High-Frequency Structural Simulator (HFSS). In the simulation, an air cavity with radiation boundary conditions is added on the top of the substrate representing the actual circumstance. Lumped ports and vertical perfect electric conductor (PEC) bridges are used as the excitation scheme where the PEC bridge connects to the ground traces and it is selected to be the reference. The port is assigned to the surface between the signal trace and the PEC bridge. Besides, the sheet inductance introduced by the lumped port is calibrated out from the simulation results. Figure 2 shows the simulated scattering parameters of the designed CPW from DC to 170 GHz. The return loss remains better than 19.6 dB while the insertion loss is <1.3 dB in the whole frequency range.

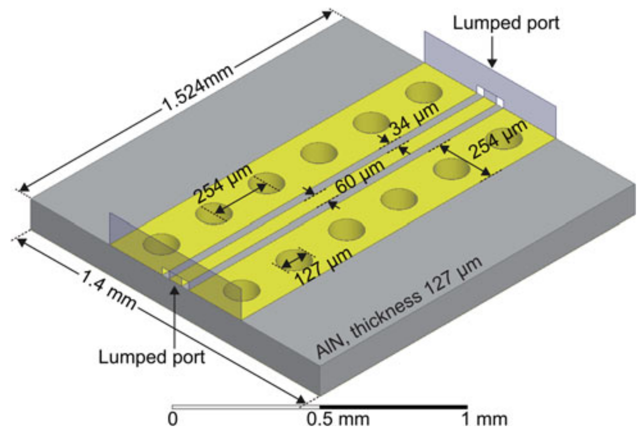

Fig. 1. Designed CPW with vias based on AlN substrate.

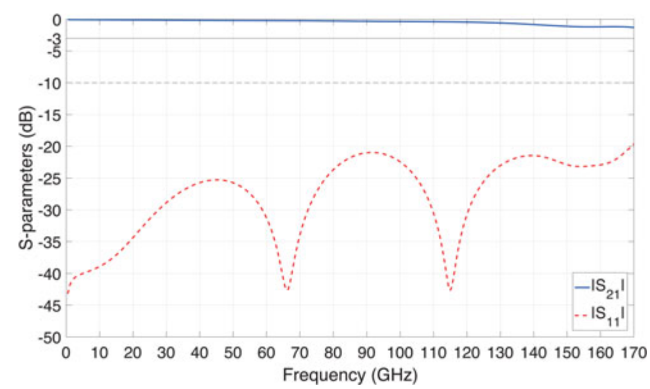

Fig. 2. Simulation results of the designed CPW.

ACPS with vias

When there is only one ground trace alongside the signal trace, it forms a GS structure. For an ACPS, the widths of the signal and ground traces are different and the electromagnetic waves exist in the gap between the signal and ground traces. In order to estimate its performance at such high frequencies, an ACPS with vias based on AlN substrate is designed by using HFSS as a part of the CPW-to-ACPS transition. Figure 3 shows the simulation structure of the designed ACPS with vias. The substrate, conductor layers, and vias are the same as they used for designing the CPW. The width of the ground trace is limited to 254 μm at the minimum due to the hollow plated vias and the width of the signal trace is 130 μm with a gap width of 50 μm.

In the simulation, an air cavity located on the top of the substrate with radiation boundary conditions is included for accuracy improvement. Wave ports are used as the excitation scheme. In order to generate the port field correctly, the ground trace as well as the bottom ground plane are touched by the edges of the wave port and they are selected to be the reference. Besides, the wave port needs to be large enough so that the

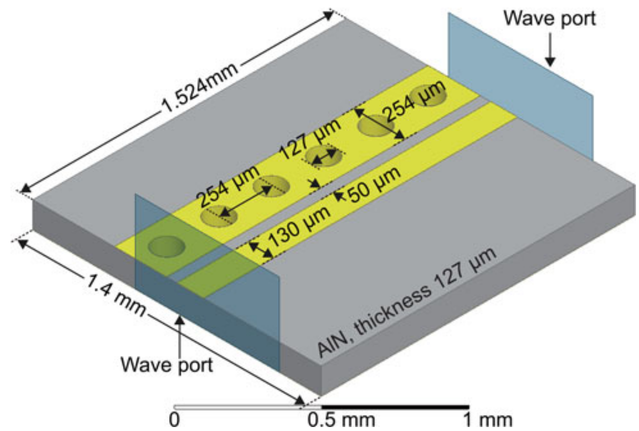

Fig. 3. Designed ACPS with vias based on AlN substrate.

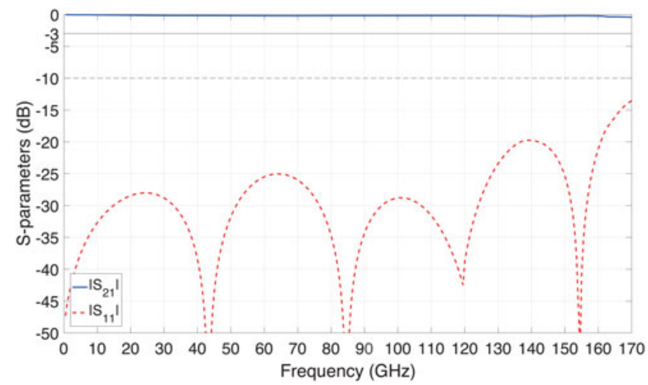

Fig. 4. Simulation results of the designed ACPS.

electromagnetic waves would not couple to the edges instead of the ground trace. The designed ACPS is simulated from DC to 170 GHz and the results are shown in Fig. 4. The simulation exhibits a return loss of 13.5 dB and an insertion loss of 0.5 dB.

CPW-to-ACPS transition with vias

Design concepts

Based on the designed CPW and ACPS, a transition between CPW and ACPS is proposed with the purpose of achieving a transmission bandwidth from DC to 170 GHz. When a CPW is connected to an ACPS, one of the ground traces has to be terminated while the signal trace and the gap need to be tapered for compensating the differences in dimensions. In order to design a transition with large bandwidth, not only the characteristic impedances need to be matched but also the propagation mode must be converted smoothly. The proposed CPW-to-ACPS transition with vias is demonstrated in detail in Fig. 5.

The CPW and ACPS in the proposed transition are designed to be 50 Ω and their dimensions are shown in Figs 1 and 3, respectively. The hollow plated vias with a diameter of 127 μm are added all the way along the ground traces in order to suppress parasitic modes and increase the transmission bandwidth of the transition. For the CPW, one of the ground traces is reserved and connected directly to the ACPS without changing its dimension while the other is terminated gradually forming a semicircle. Due to fabrication limitations, the radius of the termination is 127 μm which is 63.5 μm more than the radius of the vias. For keeping the characteristic impedance matched between the CPW and ACPS, the width of the signal trace increases from 60 to 130 μm and the width of the gap between the signal and ground traces increases from 34 to 50 μm. As a result, the signal trace is tapered in on one edge where the it moves 16 μm toward the center of the signal trace and the length of the tapered structure is 100 μm. On the other edge, the signal trace is tapered out for increasing the width where it moves 86 μm away from the center of the signal trace and the tapered structure follows the shape of the terminated ground trace forming an annular ring structure with a radius of 161 μm. Besides, the dark area on the tapered signal trace in Fig. 5 is chamfered in order to reduce the reflection caused by the termination of the ground trace and its length is 60 μm.

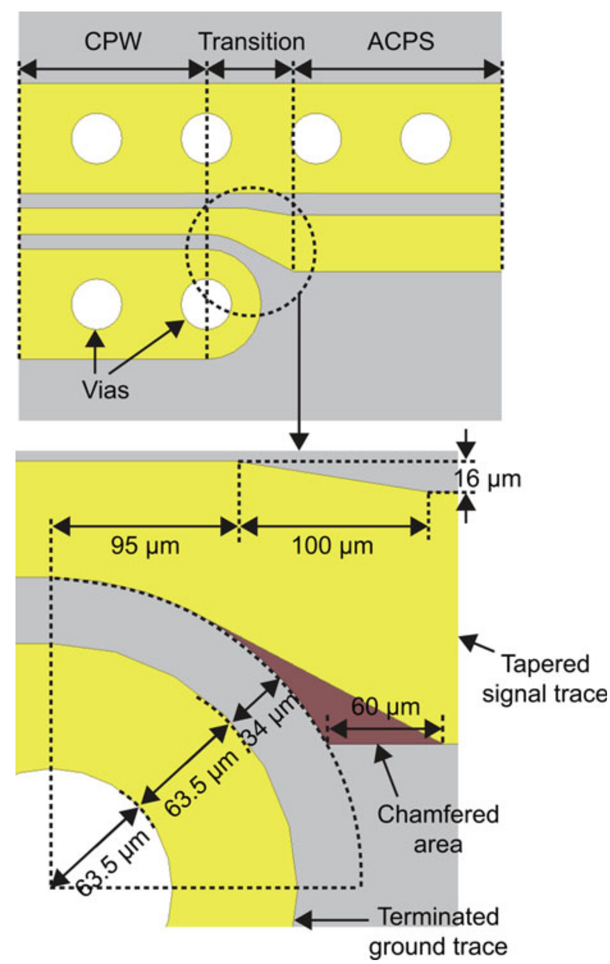

Fig. 5. Proposed CPW-to-ACPS transition with vias.

Though methods such as wire bonding bridges and air-bridge can be used for designing wideband CPW-to-CPS transitions, the substrate needs to be thick enough to avoid parasitic modes caused by the bottom ground plane. A CPW-to-CPS transition is reported in [18] with a bandwidth of 55 GHz, the substrate consists of a silicon nitride (Si_3N_4) layer with a thickness of 0.3 μm, a silicon dioxide (SiO_2) layer with a thickness of 1 μm, and a silicon (Si) layer with a thickness of 400 μm. As is explained in [28], by placing a PolyOxyMethylene (POM) absorber layer with a

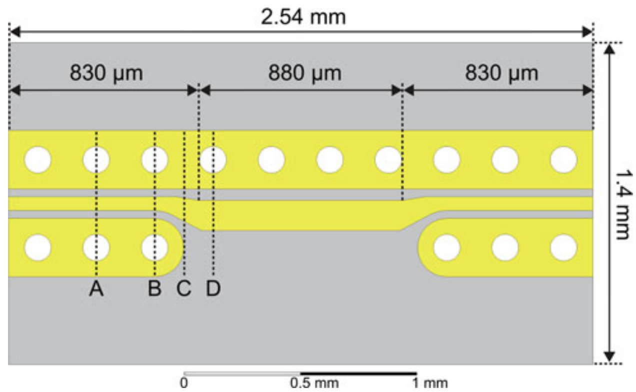

Fig. 6. Proposed CPW-to-ACPS transition in a back-to-back configuration.

thickness of 3.5 mm under an AlN substrate with a thickness of 127 μm, the parasitic modes are eliminated and the bandwidth of the proposed CPW-to-CPS transition increases from 63 to 80 GHz. In [29], a bandwidth of 110 GHz is achieved by the designed CPW-to-CPS transition which is based on a GaAs substrate with a thickness of 650 μm.

Compared with the transitions using other methods, the proposed CPW-to-ACPS transition with vias is versatile especially for applications at THz frequencies where the thick substrate, absorber layer, and extra structures on the top of the substrate have to be avoided due to the need for compact system integrations. Besides, instead of floating, the ground traces are connected to the bottom ground plane through the vias which provides lower transmission loss and better impedance matching at such high frequencies.

Transition in a back-to-back configuration

As is shown in Fig. 6, the CPW-to-ACPS transition is designed in a back-to-back configuration for easier simulation, fabrication, and measurement. There are two CPWs at the ends of the structure, an ACPS in the middle, and two transitions as interconnects. The total length and width of the AlN substrate are 2.54 and 1.4 mm, respectively.

The proposed CPW-to-ACPS transition in a back-to-back configuration is simulated in HFSS using lumped ports with vertical PEC bridges. An air cavity with radiation boundary conditions and an aluminum holder are also included in the simulation representing the measurement circumstance. The magnitude of electric field distributions at different cross-sections of the proposed CPW-to-ACPS transition at 140 GHz are simulated and shown in Fig. 7. The cross-sections correspond to the locations marked with the same letters in Fig. 6. At the beginning of CPW-to-ACPS transition, the electric fields exist mainly in the two gaps between the signal and ground traces which is a standard CPW mode. When one of the ground traces is terminated gradually and the signal trace is tapered out, the electric fields start moving from one gap to another and converting to ACPS mode at the end of the transition. The magnitude of the electric fields is slightly reduced when going through the transition which is mainly caused by the impedance mismatch, mode conversion loss, and radiation. With carefully designed structures, the proposed CPW-to-ACPS transition does not introduce high transmission losses or strong reflections and the propagation modes are converted smoothly.

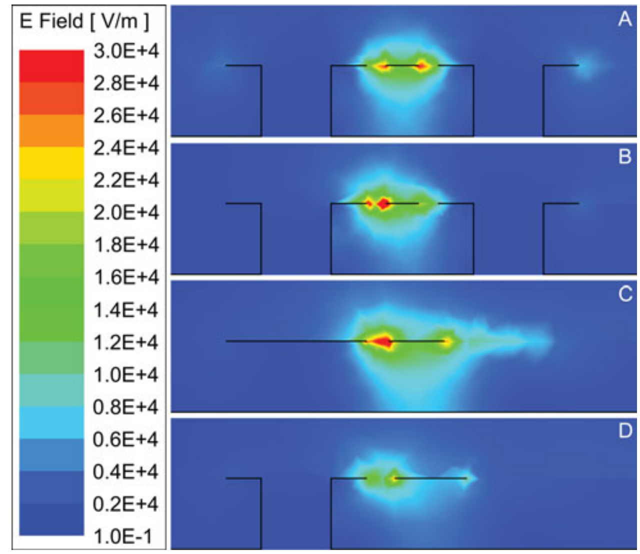

Fig. 7. Magnitude of electric field distributions at different cross-sections of the proposed CPW-to-ACPS transition at 140 GHz.

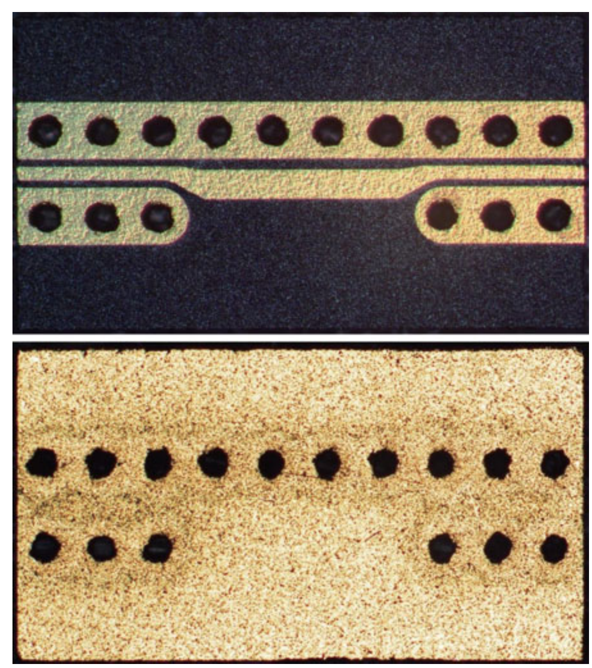

Fig. 8. Fabricated CPW-to-ACPS transition in a back-to-back configuration based on AlN substrate.

Fabrication and experimental results

In order to prove the concepts and validate the design, the proposed CPW-to-ACPS transition in a back-to-back configuration shown in Fig. 6 was fabricated based on AlN substrate. According to the information provided by the supplier, the thickness of the AlN substrate is 127 μm with a tolerance of 12.7 μm. The ϵ_r and tanδ of the AlN substrate are measured at 1 MHz and they are 8.6 and 0.001, respectively. The substrate consists of 98% AlN and 2% impurities. The thickness of the gold conductors on both sides is 1.2 μm with a tolerance of 0.24 μm. The vias going through the AlN substrate are hollow plated with gold inside.

Table 1. Comparison between this work and published GSG-to-GS transitions

Reference	Bandwidth (GHz)	Substrate	Thickness	ϵ_r	tanδ	Method	Transition type	Measurement
[18]	55	Si_3N_4	0.3 μm	8.1	0.002	Wire bonding bridge	CPW-to-CPS	Back-to-back
		SiO_2	1 μm	3.9	0.0001			
		Si	400 μm	11.9	0.005			
[28]	80	AlN	127 μm	8.6	0.001	Wire bonding bridge	CPW-to-CPS	Back-to-back
		POM	3.5 mm	3.8	0.06			
[29]	110	GaAs	650 μm	12.9	0.0016	Air-bridge	CPW-to-CPS	Back-to-back
This work	165	AlN	127 μm	8.6	0.001	Via	CPW-to-ACPS	Back-to-back

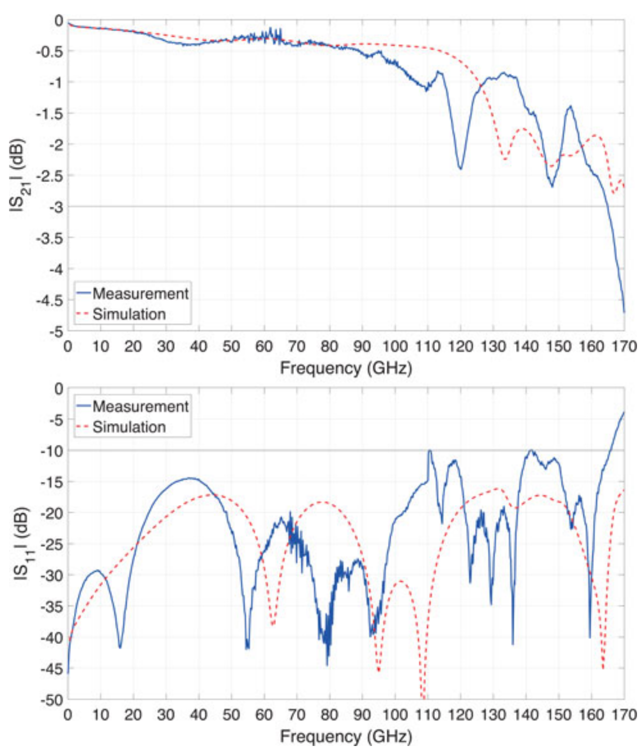

Fig. 9. Simulation (red dashed lines) and measurement (blue solid lines) results of the proposed CPW-to-ACPS transition in a back-to-back configuration.

The diameter of the vias is 127 μm with a tolerance of 25.4 μm. The top and bottom views of the fabricated CPW-to-ACPS transition in a back-to-back configuration based on AlN substrate are shown in Fig. 8.

The fabricated CPW-to-ACPS transition was characterized on-wafer using a probe station, a vector network analyzer and two GSG probes with 125 μm pitch. The two-port scattering parameters were firstly measured from DC to 110 GHz and then the setup was reconfigured for on-wafer measurement from 110 to 170 GHz.

Since the bandwidth of the transition is referred as the width of the frequency band where the return loss is better than 10 dB, the proposed CPW-to-ACPS transition in a back-to-back configuration exhibits a simulated bandwidth of 170 GHz which is shown by the red dashed lines in Fig. 9. From DC to 170 GHz, the simulated insertion loss is <2.8 dB. The blue solid lines in Fig. 9 show the measurement results of the fabricated CPW-to-ACPS transition in a back-to-back configuration. Compared with the simulation results, a reasonable agreement has been achieved. The fabricated CPW-to-ACPS transition in a back-to-back configuration provides a bandwidth of 165 GHz with an associated insertion loss of 3 dB. The differences between simulation and measurement results are mainly caused by the variation of electrical properties based on frequency for the AlN substrate as well as the fabrication tolerances, especially for the surface roughness of the gold conductors and the diameter of the vias. Besides, reconfiguring the measurement setup at high frequencies results in small step discontinuities at 110 GHz on the measured scattering parameters.

In Table 1, this work is compared with other GSG-to-GS transitions published in the literature. Wire bonding bridges are used in [18, 28] for increasing the bandwidth and in order to suppress parasitic modes either thick substrate or absorber layer is needed. Though the transition with air-bridge reported in [29] can achieve a bandwidth of 110 GHz, it requires multilayer patterning process based on thick substrate. In this work, based on the same substrate as used in [28], a bandwidth of 165 GHz has been achieved by the proposed transition with vias which is more than twice as large as the bandwidth reported in [28]. While having the largest bandwidth, the proposed CPW-to-ACPS transition is based on thin AlN substrate and it does not require extra structures on the top or absorber layer underneath which also makes the transition more compact and versatile for system integrations.

Conclusion

An ultra-wideband CPW-to-ACPS transition with vias based on AlN substrate has been presented in this work. The concepts of designing CPW, ACPS, and CPW-to-ACPS transition were explained. The effect of adding vias through the substrate was also discussed. The CPW and ACPS with vias were designed based on AlN substrate and simulated in HFSS. The designed CPW-to-ACPS transition with vias going through AlN substrate was demonstrated in detail. The proposed CPW-to-ACPS transition with vias was fabricated and measured in a back-to-back configuration. A reasonable agreement has been achieved between simulation and measurement results. The fabricated CPW-to-ACPS transition can provide a bandwidth of 165 GHz with an associated insertion loss of 3 dB. While having the largest bandwidth, the proposed CPW-to-ACPS transition is also more versatile for compact system integrations.

Acknowledgement. The work was supported in part by the EU funded project PANTHER under contract number 619411.

References

1. **Mao SG, Hwang CT, Wu RB and Chen CH** (2000) Analysis of coplanar waveguide-to-coplanar stripline transitions. *IEEE Transactions on Microwave Theory and Techniques* **48**(1), 23–29.
2. **Deal WR, Mei XB, Radisic V, Leong K, Sarkozy S, Gorospe B, Lee J, Liu PH, Yoshida W, Uyeda J and Lai R** (2010) Demonstration of a 0.48 THz amplifier module using InP HEMT transistors. *IEEE Microwave and Wireless Components Letters* **20**(5), 289–291.
3. **Radisic V, Leong K, Mei X, Sarkozy S, Yoshida W and Deal WR** (2012) Power amplification at 0.65 THz using InP HEMTs. *IEEE Transactions on Microwave Theory and Techniques* **60**(3), 724–729.
4. **Leong K, Mei X, Yoshida W, Liu PH, Zhou Z, Lange M, Lee LS, Padilla JG, Zamora A, Gorospe BS, Nguyen K and Deal W** (2015) A 0.85 THz low noise amplifier using InP HEMT transistors. *IEEE Microwave and Wireless Components Letters* **25**(6), 397–399.
5. **Urteaga M, Griffith Z, Seo M, Hacker J and Rodwell MJW** (2017) InP HBT technologies for THz integrated circuits. *Proceedings of the IEEE* **105**(6), 1051–1067.
6. **Zhurbenko V, Johansen TK, Squartecchia M, Midili V, Rybalko O, Riet M, Dupuy JY, Nodjiadjim V and Konczykowska A** (2017) Low conversion loss 94 GHz and 188 GHz doublers in InP DHBT technology, in Proceedings of Integrated Nonlinear Microwave and Millimetre-wave Circuits Workshop (INMMiC), Graz, Austria.
7. **Ye Y, Yu B, Tang A, Drouin B and Gu QJ** (2016) A high efficiency E-band CMOS frequency doubler with a compensated transformer-based balun for matching enhancement. *IEEE Microwave and Wireless Components Letters* **26**(1), 40–42.
8. **Johansen TK, Vidkjaer J, Krozer V, Konczykowska A, Riet M, Jorge F and Djurhuus T** (2008) A high conversion-gain Q-band InP DHBT subharmonic mixer using LO frequency doubler. *IEEE Transactions on Microwave Theory and Techniques* **56**(3), 613–619.
9. **Reck T, Zemora A, Schlecht E, Dengler R, Deal W and Chattopadhyay G** (2016) A 230 GHz MMIC-based sideband separating receiver. *IEEE Transactions on Terahertz Science and Technology* **6**(1), 141–147.
10. **Gnauck AH, Winzer PJ, Konczykowska A, Jorge F, Dupuy JY, Riet M, Charlet G, Zhu B and Peckham DW** (2012) Generation and transmission of 21.4-Gbaud PDM 64-QAM using a novel high-power DAC driving a single I/Q modulator. *Journal of Lightwave Technology* **30**(4), 532–536.
11. **Mardoyan H, Mestre MA, Rios-Müller R, Konczykowska A, Renaudier J, Jorge F, Duval B, Dupuy JY, Ghazisaeidi A, Jennevé P, Achouche M and Bigo S** (2016) Single carrier 168-Gb/s line-rate PAM direct detection transmission using high-speed selector power DAC for optical interconnects. *Journal of Lightwave Technology* **34**(7), 1593–1598.
12. **Jiang C, Krozer V, Bach HG, Mekonnen GG and Johansen TK** (2013) Broadband packaging of photodetectors for 100 Gb/s Ethernet applications. *IEEE IEEE Transactions on Components, Packaging and Manufacturing Technology* **3**(3), 422–429.
13. **Dong Y, Johansen TK, Zhurbenko V, Beretta A, Vannucci A and Locatelli G** (2015) A 3D hybrid integration methodology for terabit transceivers, in Proceedings of SBMO/IEEE MTT-S International Microwave and Optoelectronics Conference (IMOC), Porto de Galinhas, Brazil.
14. **Chiou HK, Chang CY and Lin HH** (1995) Balun design for uniplanar broad band double balanced mixer. *Electronics Letters* **31**(24), 2113–2114.
15. **Mao SG and Chueh YZ** (2006) Broadband composite right/left-handed coplanar waveguide power splitters with arbitrary phase responses and balun and antenna applications. *IEEE Transactions on Antennas and Propagation* **54**(1), 243–250.
16. **Wu P, Wang Z and Zhang Y** (2010) Wideband planar balun using microstrip to CPW and microstrip to CPS transitions. *Electronics Letters* **46**(24), 1611–1613.
17. **Lin S, Wang J, Zhang G and Hong J** (2015) Design of microstrip tri-mode balun bandpass filter with high selectivity. *Electronics Letters* **51**(13), 998–999.
18. **Anagnostou DE, Morton M, Papapolymerou J and Christodoulou CG** (2008) A 0-55-GHz coplanar waveguide to coplanar strip transition. *IEEE Transactions on Microwave Theory and Techniques* **56**(1), 1–6.
19. **Ding Y, Jiao YC, Fei P, Li B and Zhang QT** (2011) Design of a multiband quasi-Yagi-type antenna with CPW-to-CPS transition. *IEEE Antennas Wireless Propagation Letters* **10**, 1120–1123.
20. **Roshna TK, Deepak U, Sajitha VR and Mohanan P** (2014) Coplanar stripline-fed compact UWB antenna. *Electronics Letters* **50**(17), 1181–1182.
21. **Akiyama S, Itoh H, Takeuchi T, Kuramata A and Yamamoto T** (2005) Wide-wavelength-band (30 nm) 10-Gb/s operation of InP-based Mach-Zehnder modulator with constant driving voltage of 2 Vpp. *IEEE Photonics Technology Letters* **17**(7), 1408–1410.
22. **Lange S, Gruner M, Meuer C, Kaiser R, Hamacher M, Velthaus KO and Schell M** (2016) Low switching voltage Mach-Zehnder modulator monolithically integrated with DFB laser for data transmission up to 107.4 Gb/s. *Journal of Lightwave Technology* **34**(2), 401–406.
23. **Ogiso Y, Ozaki J, Ueda Y, Kashio N, Kikuchi N, Yamada E, Tanobe H, Kanazawa S, Yamazaki H, Ohiso Y, Fujii T and Kohtoku M** (2017) Over 67 GHz bandwidth and 1.5 V Vtt InP-based optical IQ modulator with n-i-p-n heterostructure. *Journal of Lightwave Technology* **35**(8), 1450–1455.
24. **Wu WC, Hsu LH, Chang EY, Kärnfelt C, Zirath H, Starski JP and Wu YC** (2007) 60 GHz broadband MS-to-CPW hot-via flip chip interconnects. *IEEE Microwave and Wireless Components Letters* **17**(11), 784–786.
25. **Zhou Z and Melde KL** (2008) Development of a broadband coplanar waveguide-to-microstrip transition with vias. *IEEE Transactions on Advanced Packaging* **31**(4), 861–872.
26. **Valois R, Baillargeat D, Verdeyme S, Lahti M and Jaakola T** (2005) High performances of shielded LTCC vertical transitions from DC up to 50 GHz. *IEEE Transactions on Microwave Theory and Techniques* **53**(6), 2026–2032.
27. **Bhutani A, Goettel B, Thelemann T and Zwick T** (2017) CPW-to-SL transition in LTCC technology. *Electronics Letters* **53**(9), 609–611.
28. **Dong Y, Johansen TK, Zhurbenko V and Hanberg PJ** (2017) Coplanar transitions based on aluminum nitride interposer substrate for terabit transceivers, in Proceedings of the 47th European Microwave Conference (EuMC), Nuremberg, Germany.
29. **Kim S, Jeong S, Lee YT, Kim DH, Lim JS, Seo KS and Nam S** (2002) Ultra-wideband (from DC to 110 GHz) CPW to CPS transition. *Electron Letters* **38**(2), 622–623.

Yunfeng Dong received the B.Sc. degree in Electronic Information Engineering from the Beijing University of Technology (BJUT), Beijing, China, in 2012, the M.Sc. degree in Wireless Engineering from the Technical University of Denmark (DTU), Lyngby, Denmark, in 2014, and is currently working toward the Ph.D. degree at DTU. From September 2011 to July 2012, he was an exchange student with the South-Eastern Finland University of Applied Sciences (XAMK), Mikkeli, Finland. From October 2014 to December 2014, he was a Research Assistant with the Electromagnetic Systems Group (EMS), DTU, Lyngby, Denmark. From October 2017 to November 2017, he was a visiting scholar with the Terahertz Systems Technology Group, the Technische Universität Darmstadt, Darmstadt, Germany. His current research interests include developing innovative strategies that are suitable for hybrid integration and packaging at millimeter-wave and terahertz frequencies.

Tom K. Johansen received his M.Sc. and Ph.D. degrees in Electrical Engineering from the Technical University of Denmark (DTU), Lyngby, Denmark, in 1999 and 2003, respectively. In 1999, he joined the Electromagnetic Systems Group (DTU Elektro), DTU, where he is currently an Associate Professor. From September 2001 to March 2002, he was a Visiting Scholar with the Center for Wireless Communication, the University of San Diego, San Diego, CA, USA. From November 2012 to February 2013, he spent a sabbatical with the Ferdinand

Braun Institute (FBH), Berlin, Germany. His research interests include the modeling of HBT devices, millimeter-wave and sub-millimeter-wave integrated circuit design, and reconfigurable microwave components.

Vitaliy Zhurbenko received the M.Sc. degree in Electrical Engineering from the Kharkiv National University of Radio Electronics, Kharkiv, Ukraine, in 2001, and the Ph.D. degree in Electrical Engineering from the Technical University of Denmark (DTU), Lyngby, Denmark, in 2008. In 2005, he joined DTU, where he is currently an Associate Professor. His current research and teaching interests include microwave and millimeter-wave sensing for biomedical and security applications; microwave and millimeter-wave components and integrated circuits for instrumentation applications; antennas and passive circuit design and characterization; and magnetic resonance technology.